# ANALYSIS OF GPR HYPERBOLA TARGETS USING IMAGE PROCESSING TECHNIQUES

MOHAMMAD ALI SHAHRABI and HOSEIN HASHEMI

*Institute of Geophysics, University of Tehran, Tehran, Iran.*
*hashemy@ut.ac.ir*

(Received October 23, 2020; revised version accepted September 5, 2021)

ABSTRACT

Shahrabi, M.A. and Hashemi, H., 2021. Analysis of GPR hyperbola targets using image processing techniques. *Journal of Seismic Exploration*, 30: 561-575.

The Canny edge detection method is an image processing technique that can be used to distinguish the edges of an image. This edge detection operator is mostly used for the analysis of object boundaries of images such as edge-based face recognition, edge-based obstacle detection, edge-based target recognition, image compression, etc. Ground Penetrating Radar (GPR) is a non-destructive geophysical method that is most often applied to detect underground features such as subsurface facilities, geological structures, changes in material properties, and voids and cracks. Small underground targets such as pipes and cables are expressed into radargrams as hyperbolic-shaped signatures depends on the orientation of the acquisition direction concerning the position of the object. Taking into account the large quantity of acquired GPR data during a field operation, the manual detection and localization of hyperbolas in radargrams can be time consuming and impracticable in large-scale surveys.

In this work, the applicability of the Canny edge detection operator is investigated in the GPR processing procedure. In particular, Canny edge detection is used as a processing step for the detection of hyperbolic reflections in GPR images. The open-source finite-difference time-domain (FDTD) simulator GPRMax was used to generate synthetic radargrams.

KEY WORDS: GPR processing, Canny edge detection, edge linking, velocity analysis.

0963-0651/21/$5.00 

## INTRODUCTION

As a non-destructive geophysical method, Ground Penetrating Radar (GPR) is applied for investigation of the near-surface and has been widely exploited in detecting and mapping underground utilities such as pipes and cables (Daniels, 2004). Hyperbolic curves and linear segments are two typical pattern shapes in the GPR radargram (Bruschini et al., 1998). If the cross-section size of an object is comparable to the radar pulse wavelength, a hyperbolic curve will form in the output section. Interfaces in the form of a plane between layers with different electrical impedance create a linear segment. Automatically extraction of hyperbolae from GPR data is a complicated work because GPR images are usually noisy.

The source of noise in GPR sections is consisting of system noise, the heterogeneity of the medium, and mutual wave interactions (Dou et al., 2016). Researchers have exploited extensive research in this area and have applied many different strategies to handle this topic (Xue et al., 2019; Kim et al., 2007; Bi et al., 2018). Furthermore, by fitting a hyperbola to a hyperbolic curve and obtaining the coefficients of the hyperbola's equation, the location and size of the object can be achieved by using the coefficients, which lead to calculating the average velocity of the propagated electromagnetic wave in the medium (Shihab and Al-Nuaimy, 1998). Different procedures have been applied to detect hyperbola and its features in GPR images. Windsor et al. proposed generalized Hough transform algorithms which were time-consuming in the detection of hyperbola parameters, and the accuracy depends on how much the parameters are discretized. The more discretized the parameters, the more time is required to proceed computation process (Windsor et al., 2013).

The application of machine learning methods is another way to find the hyperbola parameters. Chen and Anthony (2010) suggest a probabilistic model which is based on a classification using expectation-maximization (EM) algorithm to extract multiple hyperbolas from a GPR image. Orthogonal hyperbola fitting algorithms are more sensitive to the configuration of the given points, and their computation is expensive. The EM algorithm initiates with a general primary portion of the given points, which it is difficult to guarantee the convergence of the hyperbola fitting algorithm. In each step, the EM algorithm calls the hyperbola fitting algorithm multiple times (Chen and Anthony, 2010). Al-Nuaimy et al. (2000) extracted regions including hyperbolae with a neural network and then employed an edge detector to detect edges in the extracted regions. The parameters of hyperbolae are extracted through a generalized Hough transform. Application of EM based on Gaussian Clustering of seismic data is previously discussed by Shahrabi et al. (2015).

The use of image processing techniques on adaptive radon transform of seismic data are recently published by Zarei and Hashemi (2021). Mertens et al. (2015) applied an edge detector to extract edges from GPR images. Even though the neural network extraction method applies to complex GPR sections only the apexes of the hyperbolae are detected and other parameters of the related hyperbolae are missed. The reason is that there is no direct fitting method to apply to the identified edge points. This in turn leads to missing identification of other properties of the utilities such as the size and even the materials of them.

In this proposed manner, the general idea is to apply the synthetic model of GPR radargram consists of different kinds of simulated buried objects to obtain their characteristics. In this way, proposing a Canny edge detection algorithm and edge linking algorithms are practical to detect the edges of simulated buried objects in the GPR radargram. The propagated velocity, as well as geometrical parameters of each simulated buried object, have been calculated exploiting hyperbola curve fitting and proven formulas. The motivation for using the proposed method is its simplified and automatic approach in finding the edges of hyperbolas, while in GPR commercial softwares the user shall pick them manually to find a fitted velocity.

## GPR MODELLING

Ground-penetrating radar is ordinarily used for the non-destructive testing (NDT) of structures and transport systems (Bungey et al., 1997; Forde and McCavitt, 1993). Exploiting of GPR for NDT is just one of the many different applications of radar as a practical tool to determine the presence or absence as well as the kind of key underground features (Daniels, 1996). Fast data acquisition capability, high ability to sort out, and its good response to metallic and nonmetallic targets equally, are the main benefits of GPR. However, its main dilemma is the complexity of the nature of data and obstacles to its interpretation.

GPR interpretation is usually confined to specifying general areas of interest or just locating anomalies instead of accurate determination of the type of targets and size and exact position of them. Analytical and numerical Modelling of GPR responses plays an essential role in improving our knowledge of GPR and providing new data processing techniques and interpretation software.

Most of the proposed modeling approaches (Gianopoullis, 1997; Bergmann et al., 1998; Bourgeois, 1996) are based on the finite-difference time-domain (FDTD) method. The main reasons for such widespread use of the FDTD method are its ease of implementation in a computer program – at least at a simple introductory level and its good scalability when compared with other popular electromagnetic modeling methods such as the finite-element and integral techniques (Millard, 1998).

The FDTD technique has two main drawbacks which are: first, requiring to discretize the volume of the problem space which could lead to excessive computer memory requirements, and second, the staircase representation of curved interfaces. Taflove (1995) has provided a supreme introduction to the technique of the FDTD method and details of the FDTD method development have been discussed. It is a very difficult and almost impossible task, even for experienced scientists and engineers, to analytically address the GPR forward problems. Maxwell's equations describe any electromagnetic phenomena which are on a macroscopic scale. The first order partial differential Maxwell's equations represent mathematical relations between the fundamental electromagnetic field quantities and their dependence on their sources (Balanis, 1989). The GPR forward modeling problems are classified as an open boundary problem. Therefore, there are two issues to find a solution for GPR problems; the first one is defining an initial condition which means the excitation of the GPR transmitting antenna, and the second issue is the propagation of the resulting fields through space and reaching a zero value at infinity. The first issue is relatively easy to incorporate by ignoring the exact details of the GPR antenna. However, the second issue (i.e., the formalization of the model) cannot be easily addressed by using a finite computational space. The FDTD approach is applied to discretize both space and time continuity. It is based on the numerical solution of Maxwell's equations. It is very important to reduce the spatial and temporal discretization steps to reach a much more realistic FDTD model of the problem. The building block of the discretized FDTD grid is the Yee cell, its 3D cell structure is illustrated in Fig. 1. GPRMax is a computer program that implements the FDTD method for GPR modeling in 2D and 3D which has an easy-to-use command interface. Different dispersive materials and complex shaped targets can be modeled by GPRMax. Another feature of it is simulating unbounded space using powerful absorbing boundary conditions (Giannopoulos, 2005).

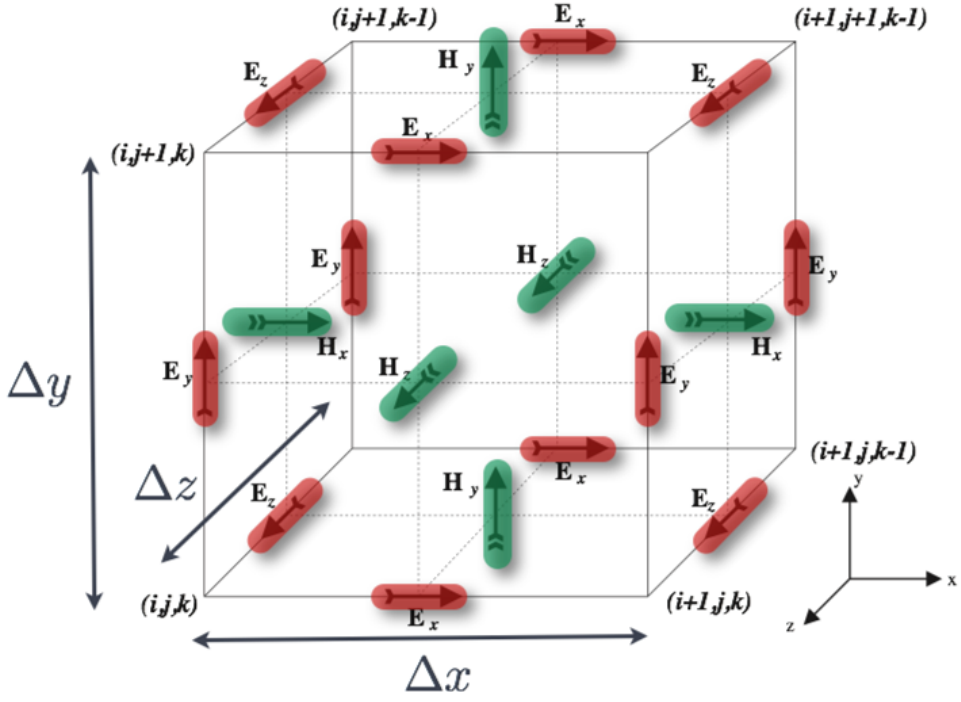


Fig. 1. The 3D Yee cell (Giannopoulos, 2005).

## CANNY EDGE DETECTION THEORY

Edge detection has many different applications in image processing such as image morphing, pattern recognition, image segmentation, image extraction which make it one of the most prominent parts of the image processing concepts. Edge detection contributes to much important information. Edge detection algorithms represent the image with contours which make it a recognizable object with its detected edges. One of the most important features of the edge detection methods is the detection of the exact edges accompanying the good object orientation in the image (Kabade et al., 2016; Canny, 1986).

Many edge detection algorithms are mainly classified into two types that are Gradient-Based algorithms and Laplacian Based algorithms. This classification is based on the order of applied derivation. The canny edge detector is a standard edge detection algorithm. Obtaining image information is the essential purpose of image processing. An image consists of different information on a scene such as the size, color, orientation of different objects present in that scene (Kabade et al., 2016; Canny, 1986).

An interesting point is that first the object is separated from the background then all the edges have to be detected to get the outline of the object. This is the reason why edge detection becomes important in computer vision and image processing. In the Canny Edge Detection Algorithm, only two thresholds for all the images are used to get a better edge map. The canny edge detector is exploited to each block of an image. However, in some smooth regions of the image detection of false edges is inevitable and the algorithm fails to detect some of the true edges. To conquest this, a block-level canny edge detector is proposed which could give better performance at each block of the image. The three main characteristics of the canny edge detection are as follows: 1. Low error rate; which means detecting edge accruing in images and there should be no response for non-edge. 2. Good Localization; which means minimizing the distance between the detected edge pixels and the actual edge. 3. Single Response; there should be one response to a single edge.

The algorithm mainly has five steps in it:

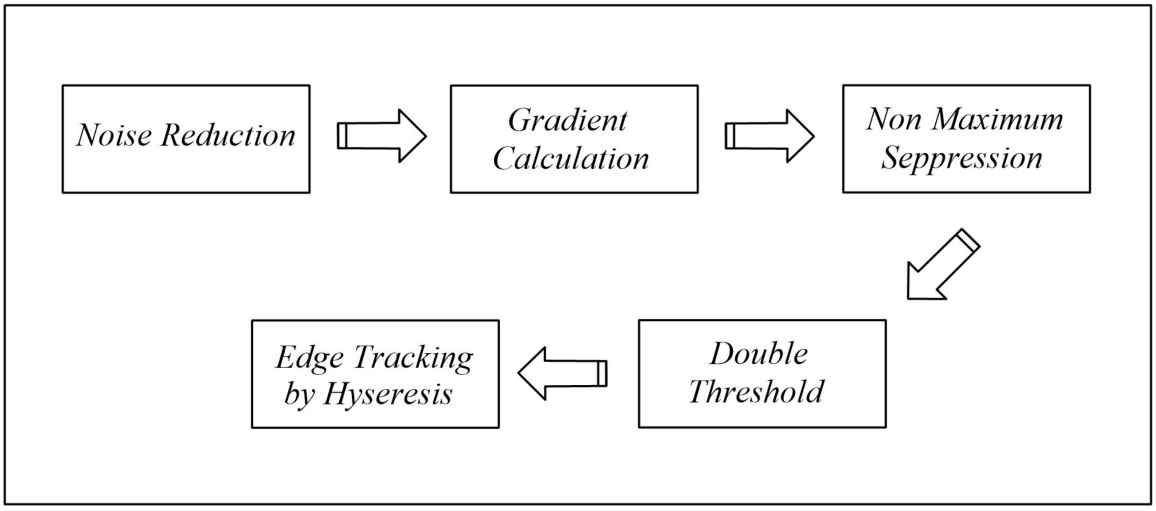


Fig. 2. Flow chart of the Canny edge detection algorithm.

Step one: *Noise Reduction*: Mathematics processing of the canny method is mostly based on derivation methods, so image noise highly affected the edge detection results. Applying Gaussian blur to smooth the image is a good way to shake off the noise on it. The image convolution technique with a Gaussian Kernel is applied to reduce the noise effects (Maini et al., 2009).

Step two: *Gradient Calculation*: In this step, the edge intensity and direction is detected by calculating the gradient of the image using edge detection operators. Edges correlated with a change in intensity of pixels. The easiest way to detect this is to apply filters that highlight this intensity change horizontally and vertically.

Step three: *Non-Maximum Suppression*: Ideally, the final image should have thin edges. Thus, we must perform non-maximum suppression to thin out the edges. The algorithm finds the pixels with the maximum value in the edge directions by going through all the points on the gradient intensity matrix (Haralick, 1984).

Step four*: Double threshold*: It means identifying three kinds of pixels (strong, weak, and nonrelevant). Pixels with a high-intensity value that surely contributes to the final edge are named strong pixels. Pixels with an intensity value neither enough to be considered as strong, nor small enough to be considered as non-relevant for the edge detection are weak pixels. Other pixels are named non-relevant for the edge. Pixels with intensity higher than the high threshold are identified as the strong pixels, and those with intensity lower than the low threshold are identified as the non-relevant pixels. All other pixels which have intensity value between both thresholds are flagged as weak and will be categorized by the Hysteresis mechanism (next step) to be considered as strong or non-relevant (Kitti et al., 2012).

Step five: *Edge Tracking by Hysteresis*: The hysteresis threshold method is employed to reach the proper edge map result. This method links between the weak and strong pixels. if and only if at least one of the pixels around the one being processed is a strong one, the hysteresis transforms weak pixels into strong ones, otherwise, they are eliminated from the map.

## METHODOLOGY

The flexibility of the GPRMax2D module allows us to create models in complicated scenarios. The GPR synthetic model is created by a flexible GPRMax2D module. The simulated GPR scan is performed by exploiting a predefined GSSI antenna model 5100. A Ricker (or Mexican Hat) waveform which is the negative, normalized second derivative of a Gaussian waveform with a center frequency of 1.5 GHz was used to excite the antenna, which was fed by a transmission line with a characteristic impedance of 50 Ohms in the GPRMax module. The features of the antenna model are similar to the commercial GPR antennas (Gianopolous, 2005). The dimensions of the antenna are 170×108×45 mm with a resolution of 1.2 mm. The step size of

the antenna movement has been chosen as 2 mm. The GSSI 1.5-GHz (Model 5100) antenna is a high-frequency, high-resolution GPR antenna that is primarily used for the evaluation of structural features in concrete: the location of rebar, conduits, and post-tensioned cables, as well as the estimation of material thickness on bridge decks and pavements. (Warren et al., 2011). The synthetic model parameters are considered to be similar to those structural features to obtain the most appropriate result.

The geometry of the problem is a 1.5×0.235×0.15 m box. The upper part is a free space of air where the antenna is located to move. The lower part of the box is half-space of concrete which its electrical properties were assumed to be $\epsilon_r = 6$ and $\mu r = 0.01$ H/m. An illustration of the used model is presented in Fig. 3. It is assumed that the antenna moves through the X-direction of the box, sending and receiving signals in each cube of the box.

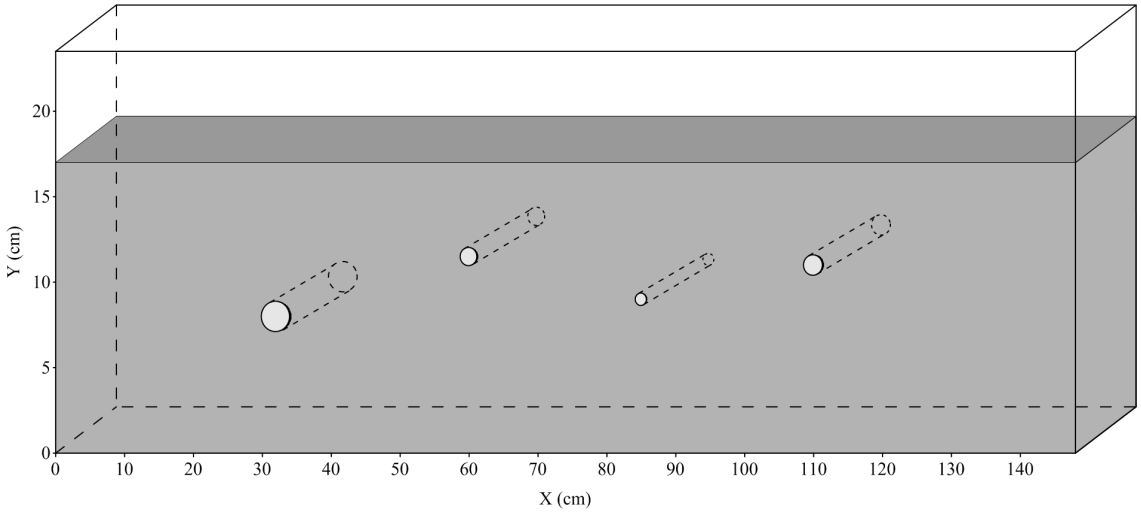


Fig. 3. The schematic model of buried objects.

Different objects consist of PVC pipe, PE pipe, metal pipe, and wood with different diameters are buried at different depths from the slab's surface. The geometry of buried objects and their parameters are illustrated in Table 1. Neither the horizontal distance between objects nor their cover depth is not fixed.

Table 1. Object parameters resulted from fitting.

| Objects\Parameters | Radiu | Depth | X location | Relative permittivity ($\epsilon_r$) F/m | Permeabilit ($\mu_r$)H/m |
|---|---|---|---|---|---|
| Object 1 | 3.5 cr | 15.5 cn | 32 cm | 1.45 | 0.0035 |
| Object 2 | 2.5 cr | 12 cm | 60 cm | 1.5 | 0.0035 |
| Object 3 | 2 cm | 14.5 cn | 85 cm | 0 | 0.005 |
| Object 4 | 2.7 cr | 12.5 cn | 110 cm | 3 | 0.001 |

In detail, applying the image processing toolbox of Matlab software, the GPR synthetic model image is first converted to grayscale by the weighted average method to reduce the intensity values of pixels. Then, using Canny Operator, edges of radar-gram find with applying different values for hysteresis thresholds and smoothing parameter of sigma. Edge pixels link together into lists of sequential edge points, one list for each edge contour. An edge contour which is named as edge list either starts or stops at an ending or a junction with another contour or edge list. contours less than 10 pixels long are discarded. Applying the polynomial fitting method on the obtained edge list matrix, the equation coefficients of each hyperbola have achieved. Fig. 4 shows a typical synthetic GPR radar-gram created by the GPR modeling module with hyperbolic signatures resulted from four different objects.

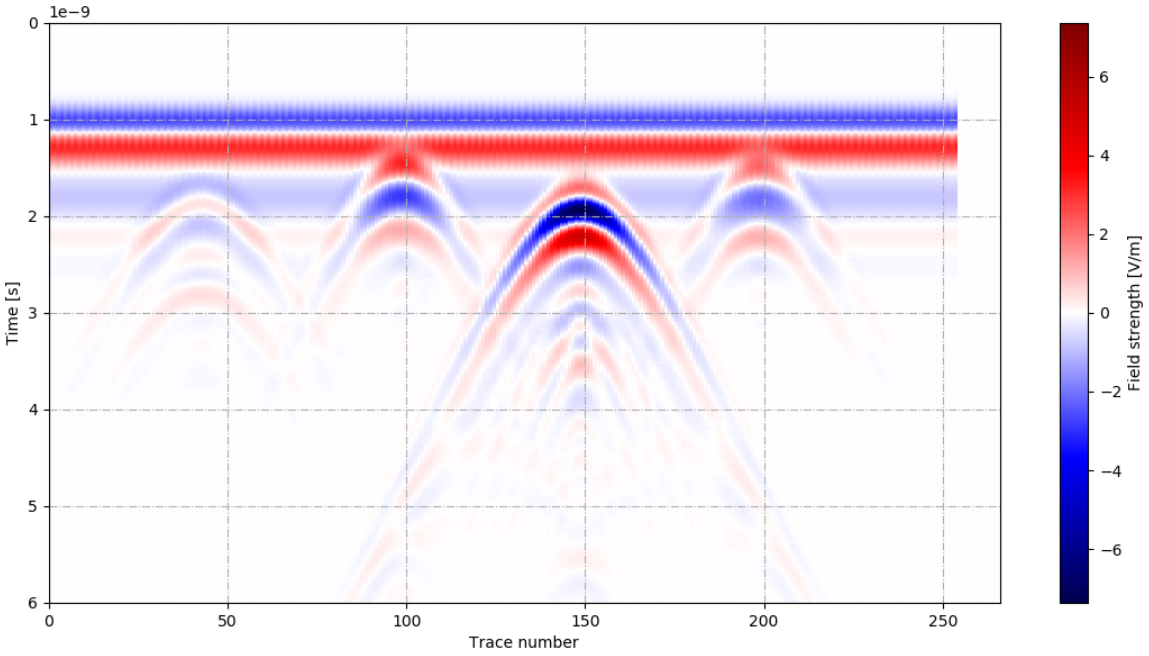


Fig. 4. GPR simulated section created by GPRMax module.

Horizontal lines and multiple hyperbolas in the model are due to the proximity of buried objects to the surface. Multiplying and ringing have been accrued when the wavelength of transmitted signals is longer than the distance of the underground anomaly to the surface (Daniel, 2004).

## Fitting Hyperbolas

Image processing techniques such as edge detection and edge linking are used to reduce the bulk of the image data to small sets of points and lines representing the edges of the reflected wavefronts from signatures that are supposed to be hyperbolic in shape. The fitting of hyperbolic equations to image data and obtaining hyperbolic coefficients is an important step in resulting underground object's characteristics. By fitting a hyperbola to such edges, one can accurately characterize the shape of this hyperbola and hence extract meaningful target-specific information. One such model is the hyperbola, but despite the importance of this stage to the interpretation of ground-penetrating radar data, the literature shows little interest in developing fitters specific to this shape.

The fitting procedure is a polynomial curve fitting method to adequately characterize the hyperbola in terms of parameters *a* and *b*, and hence providing the necessary information for target identification. The polyfit curve fitting function is based on the direct least-square method and was specifically adopted for polynomial functions and curves. The parameter values of *a* and *b* are used to synthesize a hyperbola that is cross-correlated with the detected edges to validate the fit. It can adequately deal with noisy data having missing points and is completely efficient. According to Al-Nuaimy et al. (2000) Both *a* and *b* are obtained as a result of the fitting process and its process and it becomes possible to calculate both *v* and *R* from:

$$R = b\,(a - t_0)\,/\,\mathrm{a} \quad . \tag{1}$$

Radius Estimation for Cylindrical Objects and the velocity is

$$v = 2\,b\,/\,\mathrm{a} \quad . \tag{2}$$

The values of *R, v*, and $t_0$ are converted physically to dimensions using the GPR-scan header parameters, namely range, scans-per-meter, and samples-per-scan. The depth is found from:

$$Depth = v\,t_0\,/\,2 \quad . \tag{3}$$

## RESULTS

To make it possible to extract velocity information from the hyperbolic signatures detected in GPR radar grams, both the canny edge detection and the edge linking technique are applied. The resulting technique illustrates a new stage in GPR data processing and interpretation. The stage after this one involves a polynomial fitting procedure to calculate coefficients of the second-order hyperbola. This edge detection-linking process is quite essential since the more accurately a hyperbola is identified the better the result of the curve fitting procedure would be.

In this work, in order to distinguish the object of hyperbola through zeros and ones in the output of canny edge detecting filter in Matlab, the edge detection-linking technique is used for the detection and segmentation of hyperbolic signatures since it has proven to be highly accurate, consistent, and fast. Fig. 5 shows the Canny edge detection result and how accurately the hyperbolic signatures are identified. The linking technique is then applied to the extracted points and the results can be seen in Fig. 6.

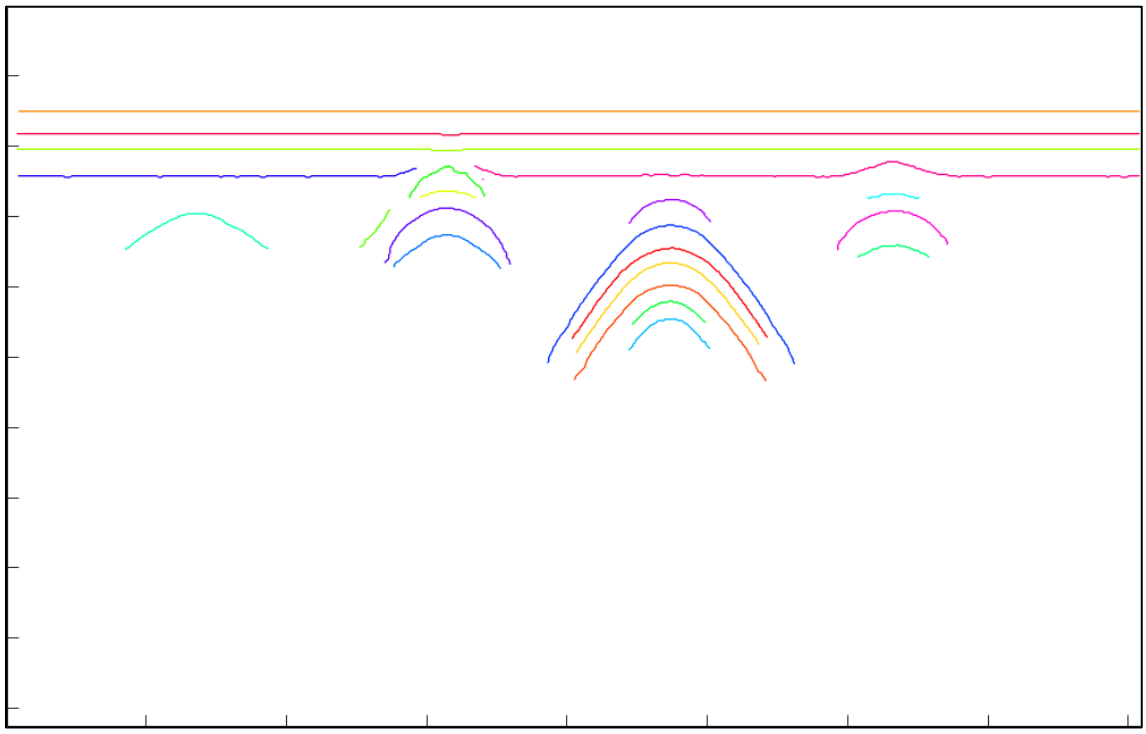

Fig. 5. Resulted hyperbola from applying the canny edge detection technique.

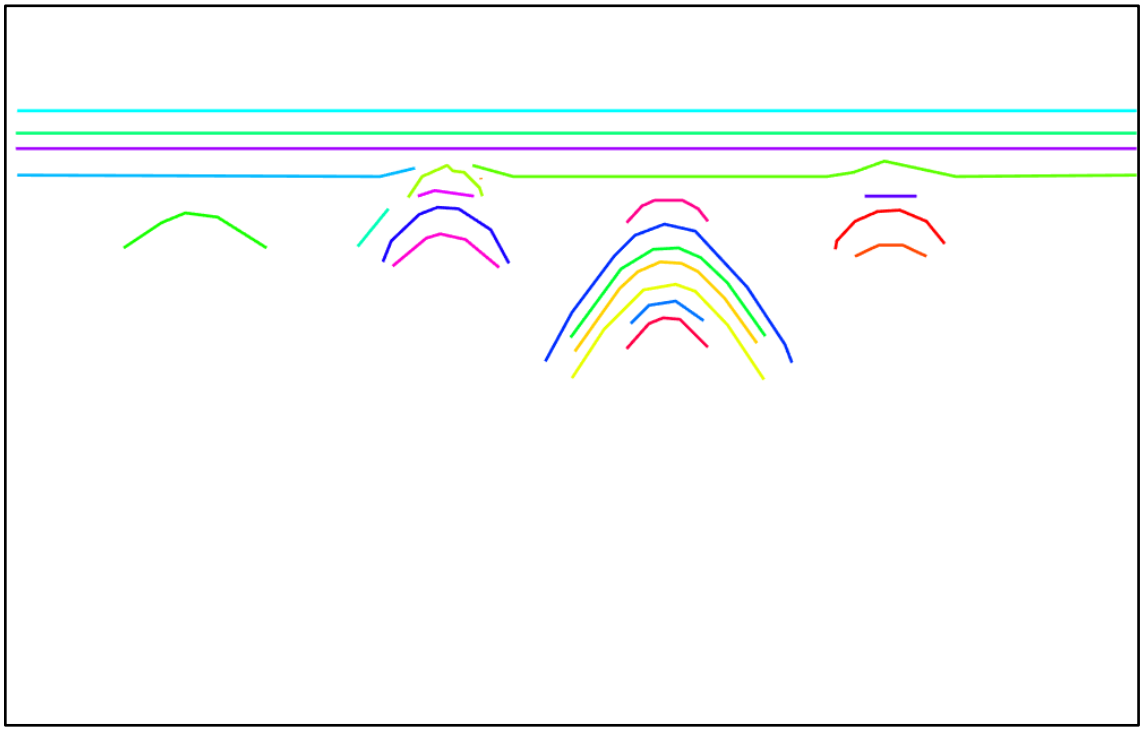

Fig. 6. Resulted hyperbola from applying the edge linking technique.

The values of the coefficients in Table 2 are obtained from the curve fitting. According to the synthetic model, the most appropriate hyperbola is the one that has the highest amplitude in the model. Therefore, among many hyperbolas that are detected for each point after the edge-linking process, the one which is proportional to the hyperbola with the highest amplitude in the synthetic model figure (Fig. 4) has been chosen. Subsequently, related coefficients of that hyperbola are considered after the curve fitting process.

Table 2. The coefficient value of hyperbola for different objects.

| | *a* | *b* | *c* ($t_0$) |
|---|---|---|---|
| Object 1 | 335.2663 | 4.76 | 0.01007 |
| Object 2 | 1992.2333 | 18.74 | 0.018691 |
| Object 3 | 3566.268 | 12.86 | 0.35602 |
| Object 4 | 6145.195 | 18.98 | 0.014994 |

For all hyperbolas, the polynomial fitter returns values for *a, b*, and $t_0$. From these values, both *R*, and *v* are calculated as in eqs. (1) and (2). It can be seen in the Table 3 that the value of velocity, Radius, and Depth for buried objects are calculated. According to Table 3, obtained values for the

Radius of objects are generally far away from the real values. Although the error rate of depth for object number one is quite acceptable, other values are too big to consider. It can be seen from the obtained results that the differences in error between the primary values and the obtained values by the method are a clear indication in favor of the inapplicability of this technique for depth and radius calculation. On the other hand, according to Table 4 results and based on the values for an error rate of velocity, one can conclude that velocity calculation applying this technique is quite acceptable. Obtained values for the velocity of each object are near to the experimental value. Among them, the best result was obtained for object 3.

Table 3. Object parameters resulted from fitting.

| Objects\Paramete | Radiu | Depth | Obtained Radius | Error rat of Radiu | Obtained Depth | Error rate Of Depth |
|---|---|---|---|---|---|---|
| Object 1 | 35 mn | 155 mn | 4.7 mm | 86.7 % | 142 mm | 8.3 % |
| Object 2 | 25 mn | 120 mn | 18.8 mm | 24.8 % | 175 mm | 45.8 % |
| Object 3 | 20 mn | 145 mn | 12.8 mm | 36 % | 2 mm | 98.6 % |
| Object 4 | 27 mn | 125 mn | 18.9 mm | 30 % | 46 mm | 63.2 % |

## CONCLUSIONS

In this paper, a novel general model is presented for the calculating of hyperbolic signature velocities resulting from different buried objects with different radius and depth. The main purpose of the process is to identify the material of the target according to the velocity value of the hyperbola. The knowledge of $v$ is quite crucial for accurately identifying buried cylindrical objects, particularly when accurate depth information is required.

Using the novel model in conjunction with our direct conic least-square fitting technique has made it possible to extract important target parameters from single radar grams. According to obtained results from the applied method, and based on the obtained velocity values it could be found that the material of the objects is as followed in Table 4.

The application of this technique on synthetic data has shown reasonable results, and it remains to extend this model to allow for out-of-plane effects where the material of the different objects in a scan area is unknown. Although the obtained values for radius and depth are not as accurate as is expected, the values for velocity can be considered as correct values.

Table 4. Pipe genders resulted from velocity values.

| Objects | Obtained velocity | Material | Experimental velocity | An error rate of velocity |
|---|---|---|---|---|
| Object | 0.0283 m/ns | PVC pipe | 0.0254 m/ns | 11.4 % |
| Object | 0.0188 m/ns | PE pipe | 0.0224 m/ns | 16 % |
| Object | 0.0000799 m/ns | Metal pipe | ~0 m/ns | - |
| Object | 0.0118 m/ns | Wood | 0.017 m/ns | 30 % |

## REFERENCES


Al-Nuaimy, W., Huang, Y., Nakhkash, M., Fang, M.TC., Nguyen, V.T. and Ericsen A., 2000. Automatic detection of buried utilities and solid objects with GPR using neural networks and pattern recognition. J. Appl. Geophys., 43: 157-165.

Balanis, C.A., 1989. Advanced Engineering Electromagnetics. John Wiley & Sons, New York.

Bergmann, T., Robertsson, J. and Holliger, K., 1998. Finite-difference modeling of electromagnetic wave propagation in dispersive and attenuating media. Geophysics, 63: 856-867.

Bourgeois, J.M. and Smith, G., 1996. A fully three-dimensional simulation of a ground-penetrating radar: FDTD theory compared with experiment. IEEE T Antenn. Propag., 34: 36-44.

Bruschini, C., Gros, B., Guerne, F., Piece, P. and Carmona, O.Y., 1998. Ground-penetrating radar and imaging metal detector for antipersonnel mine detection. J. Appl. Geophys., 40: 59-71. DOI: 10.1016/S0926-9851(97)00038-4

Bungey, J.H., Millard, S. and Shaw, M.R., 1997. Radar assessment of post-tensioned concrete. Engineer. Techn. Press, 1: 331-339.

Canny, J., 1986. A computational approach to edge detection. IEEE Transact. Patt. Anal. Mach. Intell., 8: 679-714.

Chen, H. and Anthony, G.C., 2010. Probabilistic robust hyperbola mixture model for interpreting ground penetrating radar data. Proc. Internat. Joint Conf. Neural Netw. (IJCNN), Barcelona.

Daniels, D.J., 2004. Ground Penetrating Radar. The Institution of Electrical Engineers, London. DOI: 10.1049/PBRA015E.

Daniels, D., 1996. Subsurface penetrating radar. London. The Institution of Electrical Engineers, London.

Dou, Q., Wei, L., Magee, D. and Cohn A., 2016: Real-time hyperbola recognition and fitting in GPR data. IEEE Transact. Geosci. Remote Sens., 55: 51-62.

Forde, M.C. and McCavitt, N., 1993. Impulse radar testing of structures. Proc. Inst. Civ. Engineer. Struct. Build.: 96-99.

Giannopoulos, A., 2005. Modelling ground penetrating radar by GPRMax. Construct. Build. Mater., 19: 755-762.

Gianoppollis, A., 1997. The investigation of transmission-line matrix and finite-difference time-domain methods for the forward problem of ground probing radar. Ph.D. Thesis, Univerity of York, York.

Giannopoulos, A., 2005. Modelling ground penetrating radar by GPRMax. Construct. Build. Mater., 19: 755-762.

Haralick, R., 1984. Digital step edges from zero crossings of second directional. IEEE Transact. Patt. Anal. Mach. Intell., 6: 58-68.

Kabade, A.L. and Sangam, D.V., 2016. Canny edge detection algorithm. Internat. J. Adv. Res. Electron. Communic. Engineer. (IJARECE), 5: 1292-1295.

Kitti, T., Jaruwan, T. and Chaiyapon, T., 2012. An object recognition and identification system using the Harris corner detection method. Internat. J. Mach. Learn. Comput., 2: 462-465.

Maini. R. and Aggarwal, H., 2009. Study and comparison of various image edge detection techniques. Internat. J. Image Process., (IJIP), 3: 1-11.

Mertens, L., Persico, R., Matera, L. and Lambot, S., 2015. Automated detection of reflection hyperbolas in complex GPR images with no a-priori knowledge on the medium. IEEE Transact. Geosci. Remote Sens., 54: 580-596.

Millard, S.G, Shaw, M.R., Giannopoulos, A. and Soutsos, M.N., 1998. Modelling of subsurface pulsed radar for nondestructive testing of structures. ASCE J. Mater. Civil Engineer., 10: 188-196.

Shahrabi, M.A., Hashemi, H. and Hafizi, M.K., 2016. Application of mixture of Gaussian clustering on joint facies interpretation of seismic and magnetotelluric sections. Pure Appl. Geophys., 173: 623-626.

Shihab, S. and Al-Nuaimy, W., 2005. Radius estimation for cylindrical objects detected by ground-penetrating radar. Subsurf. Sens. Technol. Applicat.: 6: 151-166. DOI: 10.1007/s11220-005-0004-1.

Taflove, A., 1995. Computational electrodynamics: the finite-difference time-domain method. Artech House, Boston.

Windsor, C., Capineri L. and Falorni P., 2013. A data pair-labeled generalized Hough transform for radar location of buried objects. IEEE Geosci. Remote Sens. Lett., 11: 124-127. DOI: 10.1109/LGRS.2013.2248119.

Warren, C. and Giannopoulos, A., 2011. Creating finite-difference time-domain models of commercial ground-penetrating radar antennas using Taguchi's optimization method. Geophysics, 76(2): Z37-Z47. DOI: 10.1190/1.3548506.

Zarei, M. and Hashemi, H., 202. Primary-multiple separation technique based on image Radon transform. Arab. J. Geosci., 14: 462.